Anal Bioanal Chem (2010) 398:1249–1255
DOI 10.1007/s00216-010-4032-x

SHORT COMMUNICATION

A simple method of surface functionalisation for immuno-specific immobilisation of proteins

R. P. Kengne-Momo · Y. L. Jeyachandran · A. Assaf · C. Esnault · P. Daniel · J. F. Pilard · M. J. Durand · F. Lagarde · E. Dongo · G. Thouand

Received: 7 May 2010 / Revised: 7 July 2010 / Accepted: 13 July 2010 / Published online: 5 August 2010

Abstract We present a new and advanced methodology, developed for surface functionalisation of gold and to study immobilisation of an immuno-specific system of proteins. A combination of electrochemical quartz crystal microbalance and Raman spectroscopy techniques allowed a complete understanding of the system starting from surface functionalisation and progressing to the functional structure analysis of immobilised proteins. A simple electrochemical procedure was formulated to prepare sulphonyl chloride terminated gold surfaces that form a strong sulphonamide bond with the receptor protein staphylococcal protein A (SpA). On the SpA grafted surfaces, the immobilisation of a human IgG and consecutive binding of an immuno-specific anti-human IgG was observed. The surface functional groups form a strong interaction with SpA without disturbing its functional properties. The native functional structure of SpA and also the IgGs was found to be retained in their immobilised state.

Keywords Surface functionalisation · Protein immobilisation · Raman spectroscopy · QCM

R. P. Kengne-Momo · Y. L. Jeyachandran · P. Daniel (✉) · F. Lagarde
Laboratoire PEC, UMR CNRS 6087, Université du Maine, A.O. Messiaen,
72085 Le Mans, France
e-mail: Philippe.Daniel@univ-lemans.fr

R. P. Kengne-Momo · E. Dongo
Laboratoire de Chimie Organique, Université de Yaoundé I,
B.P. 812 Yaoundé, Cameroon

A. Assaf · M. J. Durand · G. Thouand
Université de Nantes, UMR CNRS GEPEA 6144,
IUT Génie Biologique,
18 Bd. G. Defferre,
85035 La Roche sur Yon, France

C. Esnault · J. F. Pilard
Laboratoire UCO2M, UMR CNRS 6011, Université du Maine,
A.O. Messiaen,
72085 Le Mans, France

F. Lagarde
Université de Nantes, IUT Génie Biologique,
18 Bd. G. Defferre,
85035 La Roche sur Yon, France

Introduction

Immobilisation of proteins and antibodies, specific and non-specific interactions and structural modifications are important bio-interface mechanisms that are widely investigated in development of immuno-assays and affinity biosensors. Recent technological researches are often focussed in rapid bio-identification and improvements in sensitivity and selectivity. Among the techniques used for biological characterisation, Raman spectroscopy is one of the techniques most promising for direct detection and rapid identification [1–4]. The high responsiveness of Raman spectroscopy to conformation, orientation, chain configuration, amino acid residues and binding interactions is extremely useful in biomolecular identification [5–8]. Raman analysis with combination of a quantitative tool such as quartz crystal microbalance (QCM) could be used for biomolecules detection down to molecular scale at high precision.

However, the efficiency of biomolecules detection depends on the success of surface functionalisation and nature of biomolecules immobilisation. Polymers and self-assembled monolayer (SAM) structures are currently used for surface functionalisation [9–12]. Although, polymers are favourable for high quantity of biomolecules immobilisation, the non-specific interactions and denaturation mechanisms are predominant and could overlap specific

detection and suppress selective binding of biomolecules that sometimes lead to false positive results [9]. Furthermore, the spectral characteristics of polymers often interfere with signals from biomolecules that could cause difficulty in interpretation and identification. Using SAM, specific and selective binding of biomolecules could be achieved [10, 12]. Conventional preparation methods of SAM are a complex process that involves many experimental steps and is time consuming.

In the present work, we studied the potential of electrochemical process for functionalisation of gold surface with *para*-benzene-sulphonyl chloride. The benzene-sulphonyl chloride compounds are highly reactive to protein nitrogen that has been previously used for purification of protein and nucleic acid, and building bio-supramolecular structures [13]. For the first time, we studied the application of benzene-sulphonyl chloride for specific immobilisation of proteins. QCM and Raman spectroscopy techniques were used for the analysis of surface functionalisation and protein immobilisation.

Experimental details

Gold surface functionalisation

QCM electrodes of gold surface area 0.196 cm^2 were used as the substrates. *para*-Benzene-sulphonyl chloride functionalised QCM gold surfaces were prepared by electrochemical processes using sulphanilic acid ($C_6H_7O_3NS$, Sigma-Aldrich) as the starting precursor. The reaction was performed at ambient temperature and pressure. Sulphanilic acid, 4.3 mg, and 5.16 mg of sodium nitrite ($NaNO_2$, Sigma-Aldrich) were dissolved in 5 ml of 1 M hydrochloric acid (HCl, Sigma-Aldrich). The mixture was introduced into the electrochemical cell constituted of a QCM gold substrate as work electrode, saturated calomel electrode as reference electrode and a platinum wire as counter electrode. Cyclic voltammetry experiment (Princeton applied research, VMP2) was performed in the potential range of 0.3 to −0.25 V at a scan speed of 100 mVs^{-1} (5.5 s/scan) up to five cycles. After electrochemical reaction, the substrates were immersed in 5.2 mg phosphorous pentachloride (PCl_5, Sigma-Aldrich)/5 ml dichloromethane (CH_2Cl_2, Sigma-Aldrich) solution. Finally, the substrates were washed in CH_2Cl_2 to remove unreacted PCl_5. The functionalised gold substrates were used for protein immobilisation.

Immobilisation of proteins

An immuno-specific system of proteins such as staphylococcal protein A (SpA, Sigma p6031), human IgG (h-IgG, Sigma i4506) and anti-human goat IgG (ah-IgG, Sigma i3512) was used. Millipore water (18.2 mΩ) was used throughout the experiment. The protein solutions were prepared using phosphate buffered saline (PBS) solution of pH 7.42. The concentration of SpA solution was 50 mg/L and that of h-IgG and ah-IgG were of 1 g/L. The proteins were immobilised on the functionalised gold surfaces by consecutive immersion in SpA, h-IgG and ah-IgG solutions each for 120 min. After each step of protein immobilisation, the samples were washed in PBS and water and dried at room temperature, and Raman spectra were recorded. Additionally, the adsorption experiment of protein (SpA) was done on the pure QCM gold substrates for reference. In this case, the substrates were washed with water and PBS (pH 7.42) before using for SpA adsorption. The SpA concentration was 2 mg/ml, and adsorption was done for 120 min and 16 h. After SpA adsorption, the samples were washed in water and PBS and subjected to Raman measurements. The whole procedure was repeated in order to test the reproductibility of the results.

QCM measurements

The proteins immobilisation on functionalised gold and adsorption on pure gold surfaces were repeated for QCM measurements using a 8.95 MHz electrochemical QCM set-up (Princeton applied research, QCM922). Frequency changes were monitored for functionalisation of the gold surface of QCM electrode in the electrochemical cell. Functionalised QCM gold (BSC-gold) substrates were fitted to a liquid cell. 500 μL of PBS was initially injected into the liquid cell, and the background frequency variations were stabilised. Frequency changes for protein immobilisation were measured by injecting 10 μL of protein solution to the liquid cell. The final concentration of the proteins was around 1 mg/L for SpA and 0.02 mg/L for h-IgG and ah-IgG. In the first step, SpA solution was injected, and frequency changes were monitored. After that, the liquid cell and the gold substrates were washed in PBS and water before continuing for immobilisation of h-IgG. In reference experiment of SpA adsorption on pure gold surface, the similar final concentration of SpA (1 mg/L) was used.

For a quantitative estimation of the process, the successive coated masses were re-calculated (in nanogrammes) from the frequency shifts using Sauerbrey equation [14]:

$$\Delta F = \frac{-2{F_0}^2 \Delta m}{A\sqrt{\mu_Q \rho_Q}}$$

where

ΔF (hertz) is the change in frequency
Δm (grammes) is the added mass
F_0 is the fundamental resonant frequency of unloaded quartz (8.95 MHz)

μ_Q is the shear modulus of AT-cut quartz ($2.947.10^{11}$ g cm^{-1} S^{-2})
ρ_Q is the density of the quartz (2.648 g cm^{-3})
A is the surface area in square centimetre (0.196 cm^2).

This equation states that the decrease in frequency is linearly proportional to the increase in surface mass loading on QCM when the adsorbed films are uniform, rigid and ultra thin. Here, the recorded coated masses were very small, and the monolayer surface was roughly considered as rigid. The potential viscoelasticity of the IgG layer was neglected in order to stay in the application field of the Sauerbrey equation. Thus, the calculated Δm (nanogrammes)/ΔF (hertz) ratio=−1,066 was considered as an acceptable approximation for this study.

Raman spectroscopy

A confocal laser Raman spectrometer (XploRA, Horiba Jobin Yvon) was used for identification and characterisation. A detailed description of spectral acquisition and treatment is presented elsewhere [15]. The Raman signals were recorded in a spectral range of 400–3,100 cm^{-1} with an integration time of 300 s using a 785-nm laser excitation at 10 mW power in combination with a ×100 objective of an Olympus BX41 microscope. The Raman spectra were obtained for the gold substrates before and after functionalisation, and after each step of protein (SpA, h-IgG and ah-IgG) immobilisation. Raman spectra were also recorded for the reference sample of SpA adsorbed pure gold and the powder samples of SpA and h-IgG. Raman spectra pre-treatments were performed using standard software. A linear baseline correction jointly with a smooth function was applied to all spectra.

Results and discussion

Functionalisation of gold surface

The reaction scheme of sulphanilic acid on gold surface is presented in Fig. 1. First step is the diazotization reaction of sulphanilic acid to diazonium salt. In the next step, free radicals are formed from diazonium salt by applying an electrochemical potential in the range of +0.3 to −0.25 V. The produced free radicals readily form covalent bond with gold surface. Finally, the sulfonic acid (SO_3H) group of the bonded compound is converted to sulphonyl chloride (SO_2Cl) group by reaction in PCl_5–CH_2Cl_2 solution. The electrophilic sulphurous atom of SO_2Cl will be available for strong interaction with nucleophilic nitrogen atoms of proteins to form sulphonamide bonds.

The voltammogram of the electrochemical process is shown in Fig. 2. The reduction of diazonium salt to free radical produced a reduction band in the potential range of 0 to 0.1 V. The gold surface passivation by *para*-benzene-sulphonyl chloride layer was reached by fifth cycle where the observed current variation was very low. That is, the surface passivation of gold has reached at around 28 s (five scan cycles) where the duration of one scan cycle from potential +0.3 to −0.25 V is around 5.5 s.

The functionalisation of gold surface was monitored by QCM, and the functionalised surface was studied by Raman spectroscopy. For both experiments, the resulting spectra and measurements were very close, and in a concern of clarity, only the results of one procedure are presented and discussed here. The mass gain due to functionalisation on gold surface as a function of time is shown in Fig. 3a. A significant mass gain was observed in less than 20 s and that almost saturated by 30 s due to complete passivation of the gold surface by *para*-benzene-sulphonyl chloride as revealed in the cyclic voltammetry curves (Fig. 2). The Raman spectra measured for the QCM gold surface before and after functionalisation are shown in Fig. 3b. The functionalised gold surface showed two prominent, 1,127 and 1,595 cm^{-1}, wavenumber peaks. The bands at ~1,127 and 1,595 cm^{-1} could be associated to SO_2Cl group and benzene ring vibration mode, respectively [16, 17].

Immobilisation of proteins

QCM studies

The activity of the functionalised gold surface to specific immobilisation of proteins was studied by consecutive immobilisation of SpA (42 kDa), h-IgG (150 kDa) and ah-IgG (150 kDa). In Fig. 4, the QCM responses of SpA, h-IgG and ah-IgG immobilisation are shown along with the QCM response of SpA adsorption on pure gold surface

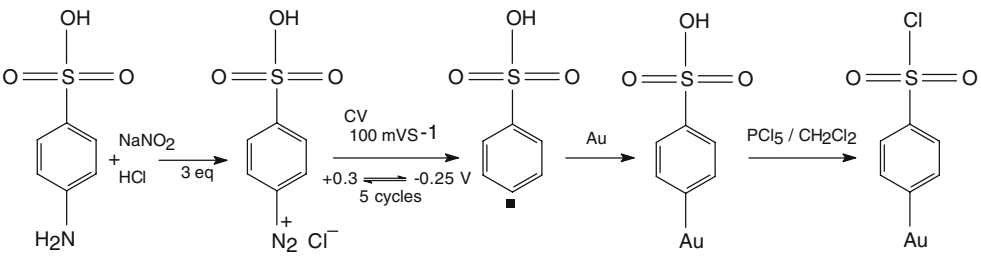

Fig. 1 Electrochemical reaction mechanism of sulphanilic acid on gold surface

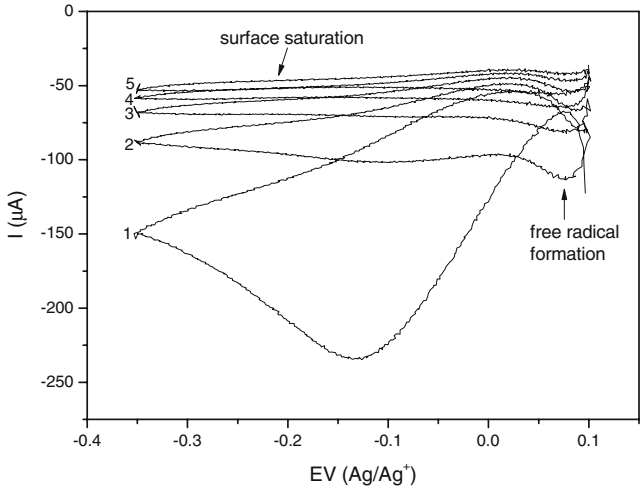

Fig. 2 Cyclic voltammetric curves of the formation of diazonium free radical and passivation of gold surface. The *numbers* of the respective scan cycle are indicated

(used as reference surface). In this case, no significant mass gain was observed for SpA adsorption, suggesting that the non-specific adsorption of SpA on pure gold surface is very low, below the detection level. On the functionalised gold surface, the mass gain during first injection of SpA solution was gradual that almost reached maximum, and the further second injection accounted for a very small increase in mass. In the following step, the first injection of h-IgG produced a sharp mass gain due to the high specific binding with SpA. The second and third injections of h-IgG produced relatively small mass addition. A significant immobilisation of h-IgG show that the immobilised SpA layer on functionalised surface retain its bioactivity. Additionally, the first injection of ah-IgG produced relatively important mass gain, probably due to recognition with h-IgG. The second and the third injections only involved little mass additions. The QCM studies show that presently used new functional surface can significantly immobilise SpA and, more importantly, preserve its bioactivity.

A quantitative estimation of the functional groups present on the gold surface and the immobilised SpA, h-IgG and ah-IgG molecules as calculated from QCM responses (Figs. 3a and 4) was found to be in the ratio of 160:2:1:1, respectively. The second experiment led to very similar values, and the discrepancy between the two calculations of the global ratio between functional groups and ah-IgG (160:1) did not exceed 3%. That is, 160 functional groups interact with two SpA molecules those in turn linked to one h-IgG molecule. The estimated surface coverages of SpA and h-IgG are around 0.2 and 0.11 molecules/nm^2, respectively, much higher than the respective calculated values of 0.007 and 0.005 molecules/nm^2 for the presented monolayer coverage.

SpA molecules consist of five receptor domains available for IgG interaction [18]. In an ideal condition with flat organisation on a surface, one SpA molecules could interact with two IgG molecules taking into account the dimension constraints. The presently observed 2:1 ratio of immobilised SpA and h-IgG molecules is one forth the value of the ideal condition. The result shows that the SpA molecules are organised as clusters in a more compact form on the functionalised surface due to strong interactions with the surface groups (160 SO_2Cl groups for 2 SpA molecules). The overlapping of receptor domain is possible in clusters hiding them for IgG interactions. The SpA clusters may be in such an organisation that exposes one of the receptor domains of two SpA molecules for h-IgG interaction. On the other hand, the 2:1:1 ratio of SpA, h-IgG and ah-IgG is

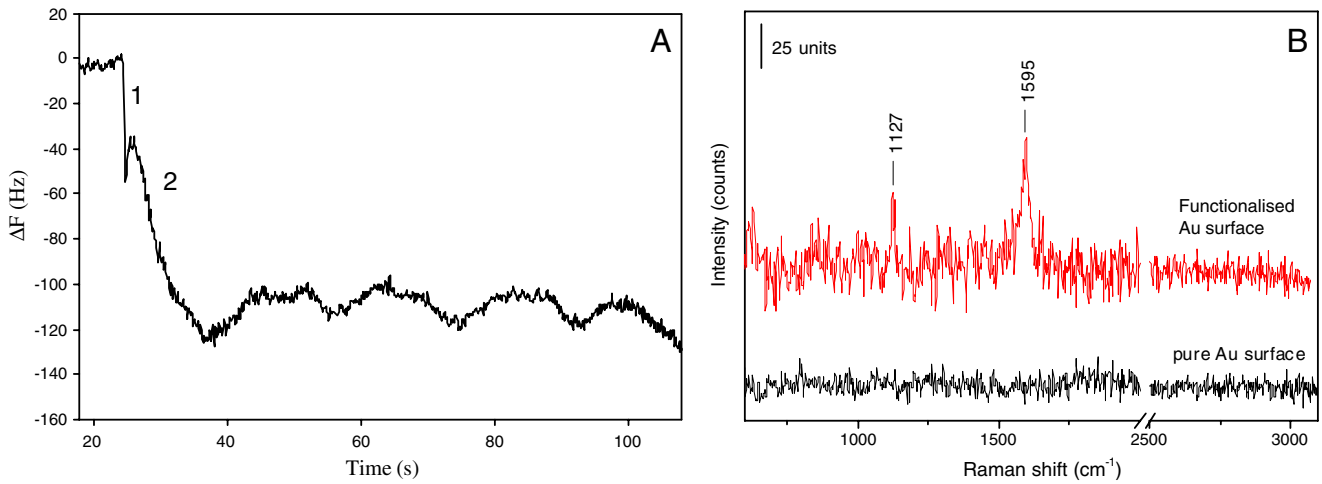

Fig. 3 **A** Quartz crystal microbalance (QCM) response during functionalisation of gold surface. The regions *1* and *2* indicate the responses to the background and functionalisation, respectively. **B** Raman spectra of a QCM gold surface recorded before and after functionalisation (300 s, 785 nm, 10 mW and ×100 objective)

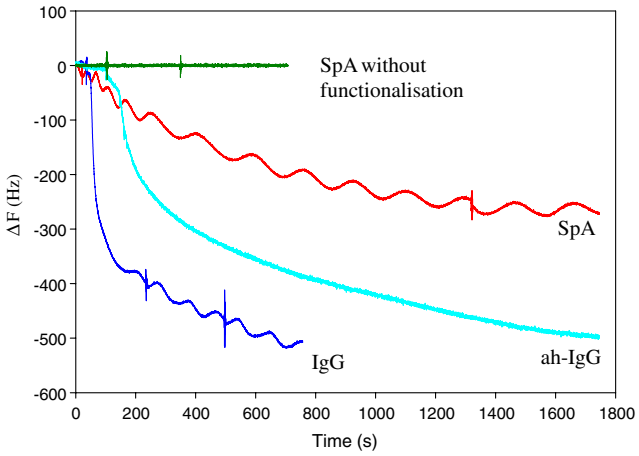

Fig. 4 Quartz crystal microbalance responses to SpA adsorption on pure gold surface and immobilisation of SpA and h-IgG on functionalisation gold surface. The first, second or third injection of protein solution are indicated in the curves

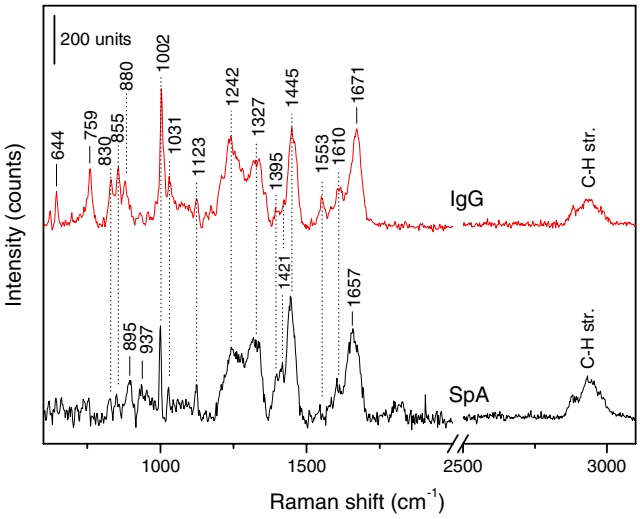

Fig. 5 Raman spectra of SpA and h-IgG powder samples (300 s, 785 nm, 10 mW and ×100 objective)

an interesting value in terms of describing specific and non-specific interactions. It could be said that the observed h-IgG immobilisation on SpA layer is through specific interaction. In the other case of non-specific interactions, a much higher immobilisation of h-IgG is expected because non-specific interactions occur irrespective of the bioactivity or organisation of immobilised SpA molecules.

Raman studies

Raman spectroscopy was used for direct identification and characterisation of the specifically immobilised SpA, h-IgG and ah-IgG layers on functionalised gold surface and adsorbed SpA on pure gold surface. Raman spectra were also recorded for pure SpA and h-IgG powder samples as reference of their native structure.

The spectra of SpA and h-IgG powder samples are shown in Fig. 5. The amide I band around 1,657 cm^{-1} and a relatively higher intense band at 1,327 cm^{-1} in the amide III region were observed in SpA spectrum that are related to its characteristics α-helix secondary structure [5, 8, 19]. SpA spectrum also featured a vibration band around 937 cm^{-1} associated with rocking vibration (ρ_{CH3}) of CH_3 terminal groups of α-helix structure [19]. The predominant β-sheet structure in h-IgG was identified by the characteristics amide I band around 1,671 cm^{-1} and a higher intense band at 1,242 cm^{-1} in the amide III region [5, 8]. The other vibration bands generally associated with proteins structure are assigned as follows from the literature [19–22]. The stretching vibration bands (ν_{CH}) of aliphatic side-chains were observed around 2,860 to 2,940 cm^{-1}. The bending band (δ_{CH2}) was observed around 1,445 cm^{-1}. Vibration bands associated with phenylalanine amino acid residue were observed around 1,610 and 1,002 cm^{-1}. The bands associated with tyrosine were observed around 853 (buried), 830 (exposed), 760 and 644 cm^{-1} (skeletal). Tryptophan (indole rings) residue bands were observed around 1,553 and 1,421 cm^{-1}. The band at 1,395 cm^{-1} could be assigned to δ_{CH3} vibration and that around 895 and

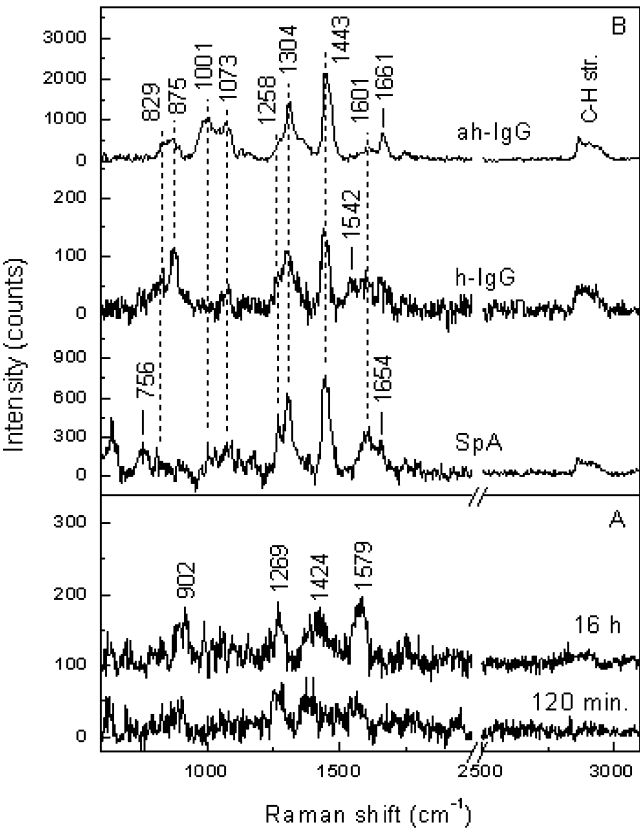

Fig. 6 Raman spectra of the proteins. **A** SpA adsorbed for 60 min and 16 h on pure gold surface. **B** SpA, h-IgG and ah-IgG consecutively immobilised for 120 min on functionalised gold surface (300 s, 785 nm, 10 mW and ×100 objective)

880 cm^{-1} to ρ_{CH2}. Backbone skeletal $\nu_{C\text{-}C}$ vibration bands were also observed around 1,123 and 1,031 cm^{-1}.

Raman spectra of immobilised protein layers on functionalised gold and adsorbed SpA on pure gold surfaces are shown in Fig. 6. The non-specific adsorption of SpA on pure gold surface was found to be very low to produce any distinct spectral features. The SpA adsorption spectra (Fig. 6a) for both 120 min and 16 h adsorption time showed broad vibration bands centred around 1,579, 1,424, 1,269 and 902 cm^{-1} that could be accounted to the presence of amide and side-chain groups.

Despite small shifts in band positions and in peaks intensities compared to reference spectra, the immobilised SpA on functionalised gold surface, specifically interacting h-IgG and immuno-specifically immobilised ah-IgG, was rather clearly identified in Raman spectra (Fig. 6b). Actually, from a theoretical point of view, the Raman shift observed can be explained because it is strongly connected to the force constant of a bond (a rough approximation suggests that the frequency is connected to force constant and mass of the atom/molecule by $\omega = \sqrt{k/m}$) and consequently influenced by the environment of atoms concerned in the bonds or involved molecular groups. The calibration on the Rayleigh line was done before each experiment (which excluded an experimental error for the 'zero frequency'), then the shift in Raman profiles could be attributed to the modification of the local structure of each entities.

The spectra (Fig. 6b) featured the prominent functional bands of proteins with reference to the spectra of proteins powder (Fig. 5). The vibration bands of amide I of α-helix (SpA, 1,654 cm^{-1}) and β-sheet (IgGs, 1,661 cm^{-1}) and amide III (1,304–1,258 cm^{-1}) were well-resolved. The alkyl side-chains bands of ν_{CH} (2,860 to 2,940 cm^{-1}), δ_{CH2} (1,443 cm^{-1}) and ρ_{CH2} (875 cm^{-1}) were observed. The vibration bands of amino acid residues such as phenylalanine (1,001 and 1,601 cm^{-1}), tryptophan (1,542 cm^{-1}) and tyrosine (829 and 756 cm^{-1}) were identified. $\nu_{C\text{-}C}$ vibration band (1,078 cm^{-1}) of the backbone structure was also observed around 1,078 cm^{-1}. Raman intensity relies to the polarisability of the molecule or compound, and then it means that a band intensity can depend on the orientation of the molecule relative to the incident laser polarisation. Intensity can also be related to concentration of molecular entities in a compound. Consequently, when compared, for instance in this study, the reference spectra of IgG under powder state (Fig. 5), to immobilised state on surfaces (Fig. 6b), a rather strong difference between the two spectra is usually observed. This could explain, for example, the quasi-disappearance of the 1,671 cm^{-1} peak, while other important characteristic peaks (1,443, 1,304 and 875 cm^{-1}) still appeared on both Raman profiles and gave evidence of the IgG presence on the surface. Considering all these theoretical aspects, the Raman spectra of the immobilised proteins on functional gold surface showed that the proteins retained their native functional structure after immobilisation.

Conclusions

A new simple method in electrochemical surface functionalisation of gold with *para*-benzene-sulphonyl chloride was formulated. Immuno-specific binding of staphylococcal protein A, human IgG and anti-human IgG on the functionalised gold surfaces was demonstrated. The surface functionalisation methodology is anticipated to be applied to immobilise all type of biomolecules more efficiently.

Moreover, in this study, conventional Raman spectroscopy was identified as a good tool to follow and characterise each step of the process. Indeed, without any enhancement method (for instance, surface enhanced Raman scattering process), it was still possible to give evidence of the SpA, IgG and anti-IgG presence on thin monolayer surfaces.

Acknowledgement The presented work was supported by the grant RMB–BIORAM booked by the Region des Pays de la Loire, Le conseil Général de la Vendée, La Ville de la Roche sur Yon.

References

1. Hutsebaut D, Vandroemme J, Heyrman J, Dawyndt P, Vandenabeele P, Moens L, de Vos P (2006) Raman microspectroscopy as an identification tool within the phylogenetically homogeneous '*Bacillus subtilis*'-group. *Syst Appl Microbiol 29:650–660*
2. Ibelings MS, Maquelin K, Endtz HP, Bruining HA, Puppels GJ (2005) Rapid identification of *Candida* spp. in peritonitis patients by Raman spectroscopy. Clin Microbiol Infect 11:353–358
3. Maquelin K, Kirschner C, Choo-Smith LP, Ngo-Thi NA, van Vreeswijk T, Stammler M, Endtz HP, Bruining HA, Naumann D, Puppels DJ (2003) Prospective study of the performance of vibrational spectroscopies for rapid identification of bacterial and fungal pathogens recovered from blood cultures. J Clin Microbiol 41:324–329
4. Yang H, Irudayaraj J (2003) Rapid detection of foodborne microorganisms on food surface using Fourier transform Raman spectroscopy. J Mol Struct 646:35–43
5. Cai S, Singh BR (2004) A distinct utility of the amide III infrared band for secondary structure estimation of aqueous protein solutions using partial least squares methods. Biochemistry 43:2541–2549
6. Jenkins AL, Larsen RA, Williams TB (2005) Characterization of amino acids using Raman spectroscopy. Spectrochim Acta A 61:1585–1594
7. Tuma R (2005) Raman spectroscopy of proteins: from peptides to large assemblies. J Raman Spectrosc 36:307–319
8. Paquin R, Colomban P (2007) Nanomechanics of single keratin fibres: a Raman study of the α-helix to β-sheet transition and the effect of water. J Raman Spectrosc 38:504–514

9. Volden S, Zhu KZ, Nyström B, Glomm WR (2009) Use of cellulose derivatives on gold surfaces for reduced nonspecific adsorption of immunoglobulin G. Colloids Surf B Biointerfaces 72:266–271
10. Limbut W, Kanatharana P, Mattiasson B, Asawatreratanakul P, Thavarungkul P (2006) A comparative study of capacitive immunosensors based on self-assembled monolayers formed from thiourea, thioctic acid, and 3-mercaptopropionic acid. Biosens Bioelectron 22:233–240
11. Chen H, Lee M, Choi S, Kim J-H, Choi H-J, Kim S-H, Lee J, Koh K (2007) Comparative study of protein immobilization properties on calixarene monolayers. Sensors 7:1091–1107
12. Kim H, Park JH, Cho I-H, Kim S-K, Park SH, Lee H (2009) Selective immobilization of proteins on gold dot arrays and characterization using chemical force microscopy. J Colloid Interface Sci 334:161–166
13. Seth AK, Jay E (1980) A study of the efficiency and the problem of sulfonation of several condensing reagents and their mechanisms for the chemical synthesis of deoxyoligoribonucleotides. Nucleic Acids Res 8:5445–5460
14. Sauerbrey G (1959) Verwendung von schwing-quarzen zur wagung dunner schichten und zur mikrowagung. Zeitchrift Phys 155:206
15. Daniel Ph, Picart P, Bendriaa L, Sockalingum GD, Adt I, Charrier Th, Durand MJ, Ergan F, Manfait M, Thouand G (2008) Effects of toxic organotin compounds on bacteria investigated by micro-Raman spectroscopy. Spectrosc Lett 41:19–28
16. Boyle TJ, Andrews NL, Alam TM, Tallant DR, Rodriguez MA, Ingersoll D (2005) Speciation in the $AlCl_3/SO_2Cl_2$ catholyte system. Inorg Chem 44:5934–5940
17. Lu Y, Chen J, Li F, Xue G (2001) Enhancing effect of chemically reduced gold on surface Raman scattering for organic sulfides chemisorbed on iron. J Raman Spectrosc 32:881–884
18. Sjoholm I (1975) Protein A from *Staphylococcus aureus*: spectropolarimetric and spectrophotometric studies. Eur J Biochem 51:55–61
19. Edwards HGM, Farwell DW, Williams AC, Barry BW, Rull F (1995) Novel spectroscopic deconvolution procedure for complex biological systems: vibrational components in the FT-Raman spectra of ice-man and contemporary skin. J Chem Soc Faraday Trans 91:3883–3887
20. Naumann D (2001) FT-Infrared and FT-Raman spectroscopy in biomedical research. Appl Spectrosc Rev 36:239–298
21. Overman SA, Thomas GJ Jr (1998) Novel vibrational assignments for proteins from Raman spectra of viruses. J Raman Spectrosc 29:23–29
22. De Gelder J, De Gussem K, Vandenabeele P, Moens L (2008) Reference database of Raman spectra of biological molecules. J Raman Spectrosc 38:1133–1147